FINITE ELEMENTS OF MULTISCALE MIXTURES (FE2M): THEORY, NUMERICAL IMPLEMENTATION, AND ANALYSES OF SIZE EFFECTS

Ashkan Almasi (1), Tim Ricken (2), David M. Pierce (1,3)

(1) Department of Mechanical Engineering, University of Connecticut, Storrs, CT, USA
(2) Institute of Structural Mechanics and Dynamics in Aerospace Engineering, University of Stuttgart, Stuttgart, Germany
(3) Department of Biomedical Engineering, University of Connecticut, Storrs, CT, USA

INTRODUCTION

We present a multi-scale finite element (FE) framework for modeling fluid saturated materials with a porous microstructures. Mixture theory and the theory of porous media both play an important role in many diverse areas of engineering, including the biomechanics of soft tissues (e.g. liver, brain, and cartilage), as well as coupled problems in material science and environmental sciences. The remarkable macro-mechanics of soft tissues derive from the complex micro-mechanics of their constituents, e.g. proteoglycans, collagens, and electrolytic fluid, and their interactions, thus multiscale models arise naturally. To facilitate mechanistic understanding and improved analyses (e.g. of experimental results) of the multi-scale mechanics of soft tissues we aimed to establish a computational framework specific to fluid-saturated, fibrous soft tissues and engineered materials.

We implemented a 3-D mutiscale framework within FEBio (Version 3.5.1, University of Utah) combining mixture theory [1] and the FE²-method [2] (i.e. finite elements of multiscale mixtures or FE2M) to solve two-scale, non-linear, coupled, and time dependent boundary value problems (BVPs) for poro-hyperelastic, fluid-saturated porous media. We attached a representative volume element (RVE) of the microstructure at each material point of the macrostructure and performed discretizations of the BVPs on both macro- and micro-scales. After successful implementation of this algorithm in 3-D nonlinear FEs, we investigated the effect of the microstructural RVE size with respect to the macrostructural model.

METHODS

Theory. We write the pull back of the balance of linear momentum of the mixture (from the current to reference configuration \mathcal{B}_{0S}) as

$$\int_{\mathcal{B}_{0S}} \operatorname{Div} \left(\mathbf{P}_{E}^{S} - p \, \mathbf{F}_{S}^{-T} J_{S} \right) dV_{0S} = \mathbf{0}, \tag{1}$$

where P_E^S is the first Piola-Kirchhof solid extra stress, p is the fluid pressure, F_S and J_S are the deformation gradient and Jacobian of the solid. We

write the corresponding balance of mass of the mixture as

$$\int_{\mathcal{B}_0} \text{Div } \left[(n^F \mathbf{w}_{FS} + \mathbf{x}_S') \mathbf{F}_S^{-T} J_S \right] dV_{0S} = 0, \tag{2}$$

where $n^{\rm F}$ is the current volume fraction of the fluid, $\mathbf{w}_{\rm FS}$ is the filtration velocity, and $\mathbf{x}_{\rm S}'$ denotes the velocity of a material point of the solid.

Numerical implementation. To solve the partial differential equations governing the macroscopic BVP, (1) and (2), we used the finite element method twice. We first provide macroscopic quantities, calculated from an intermediate solution of the macroscopic FE model, as boundary conditions (BCs) on the microscopic RVE, i.e. the deformation gradient \overline{F}_S and the gradient of pressure times the volume fraction of the fluid $\operatorname{Grad}(n^Fp)$. After solving the microscopic FE model with these BCs, we evaluate the macroscopic material tangent \overline{A} and measures \overline{P} , $\overline{(E_S)'_S} \cdot C_s J_S$, $n^F w_{FS}$ (first P-K stress, Green Lagrange strain rate, right Cauchy-Green tensor, respectively) at each Gauss integration point by a volume averaged solution of the underlying RVE. We perform computational homogenization of an arbitrary microscale quantity • over a RVE or over a representative surface element in order to calculate its macroscopic counterpart • following

$$\langle \bar{\bullet} \rangle \approx \frac{1}{V_{0S}} \int_{\mathcal{B}_{0S}} \bullet \ dV_{0S} \,, \quad \lfloor \bar{\bullet} \rfloor \approx \frac{1}{A_{0S}} \int_{\partial \mathcal{B}_{0S}} \bullet \ dA_{0S} \,, \eqno(3)$$

where V_{0S} and A_{0S} are reference volumes and areas respectively.

Numerical analyses of size effects. We considered single-scale models as benchmark solutions for comparison to corresponding solutions from equivalent two-scale models, see Fig. 1. In Fig. 1 we illustrate the scale separation in the macrostructure, meaning that each cell in a single-scale model is equivalent to an RVE (considering we have periodically repetitive cells). The shaded region in the single-scale model is equivalent to the shaded element in the two-scale model, i.e we solve an RVE for each Gauss point within each element of the macrostructure. To study the size effect we use the same RVE in progressively larger macrostructures, thus increasing the difference in scales, and compare results obtained from single and two-scale models for displacement, stress, and fluid pressure.

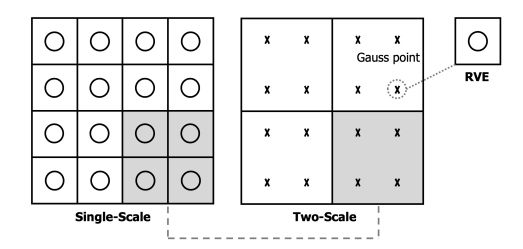


Figure 1: Schematic comparison of single-scale vs. two-scale models.

Single-scale models as benchmark solutions. We considered 3-D square plates with circular holes of length 4L, 12L, and 18L with $L=0.4\,\mathrm{mm}$; thickness $t=0.04\,\mathrm{mm}$; and radius of holes $r=0.04\,\mathrm{mm}$, see Figs. 2(a)-(c). We subjected the plates to traction $T_x=10\,\mathrm{MPa}$ and allowed that surfrace to freely drain. We used a biphasic, neo-Hookean model with properties $E=100\,\mathrm{MPa}$, $\nu=0.3$, $K_d=1e-6\,\mathrm{mm}^4/(\mathrm{Ns})$ and extracted the numerical results at time $t=1\,\mathrm{s}$. We used eight-node hexahedral elements for all finite element models.

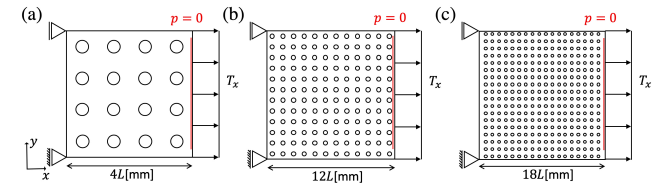


Figure 2: Single-scale finite element models: (a) Macro 1 $(4L \times 4L \times t)$, (b) Macro 2 $(12L \times 12L \times t)$, and (c) Macro 3 $(18L \times 18L \times t)$.

Corresponding two-scale models. We considered 3-D square plates of lengths nL with n=4,12,18 and $L=0.4\,\mathrm{mm}$, and thickness $t=0.04\,\mathrm{mm}$ (for the macro-scale models), see Fig. 3(a). We subjected the macro-scale models to the same BCs as the single-scale models above. For the microstructural RVEs we considered a 3-D square plate of length $L=0.4\,\mathrm{mm}$ and thickness $t=0.04\,\mathrm{mm}$ with a circular hole $r=0.04\,\mathrm{mm}$ (using 1160 elements and 1968 nodes and the same material model as above), see Fig. 3(b). We detail the number of nodes, elements, and holes for both single-scale and two-scale (macro-scale) models in Table 1.

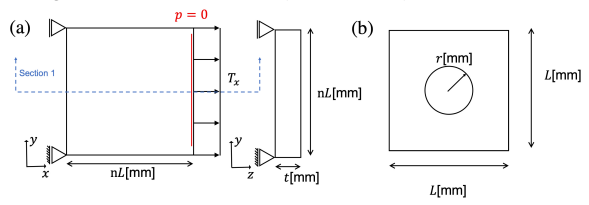


Figure 3: Two-scale finite element models: (a) macro-scale 3-D plate $(nL \times nL \times t)$ and (b) micro-scale RVE $(L \times L \times t)$.

Table 1: Number of nodes/elements in single- and two-scale models.

		Macro 1	Macro 2	Macro 3
Single-scale	Nr nodes	30,003	155,673	348,141
	Nr elements	18,560	101,376	227,412
	Nr holes	16	144	324
		Macro 1	Macro 2	Macro 3
Two-scale	Nr nodes	27	147	300
	Nr elements	8	72	162

RESULTS

In Fig. 4 we show the comparison between single-scale and two-scale models based on volume integrals, considering the traction plus free-draining surface boundary conditions. In Fig. 5 we show the convergence plot in $\|e\|_2$ for fluid pressure (n=4,12,18 and L=0.4 mm). For Macro 1, 2, and 3 (Fig.4(a), (c), and (e)), the results of the total Cauchy stress for our two-scale models showed excellent agreement with the single-scale (benchmark) solutions. As the difference in length scales increases between the macrostructure and the microstructural RVE, the error in the fluid

pressure decreases significantly to 2.8% and 1.6% for Macro 2 (Fig. 4(d)) and Macro 3 (Fig. 4(f)), respectively.

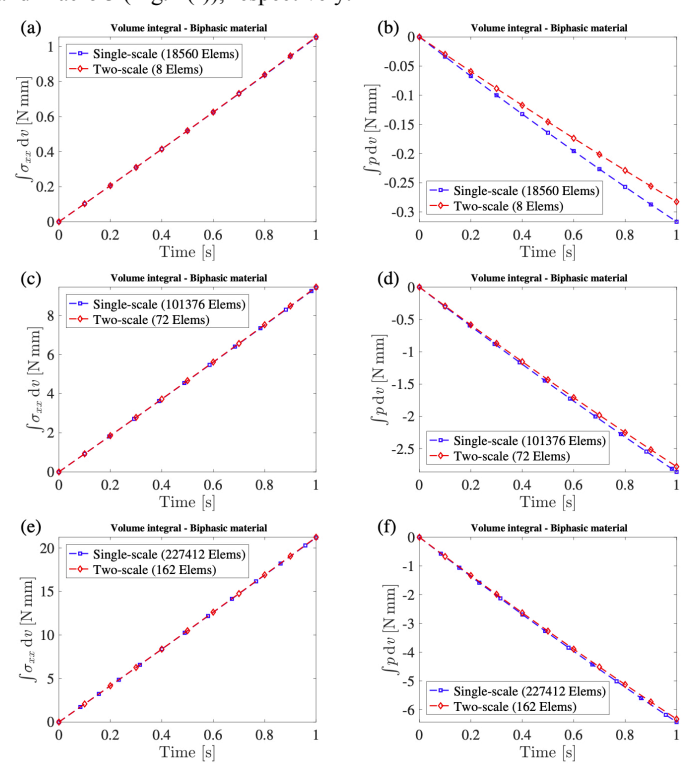


Figure 4: Single- vs. two-scale models based on volume integrals: total Cauchy stress (σ_{xx}) for (a) Macro 1, (c) Macro 2, (e) Macro 3; and fluid pressure for (b) Macro 1, (d) Macro 2, (f) Macro 3.

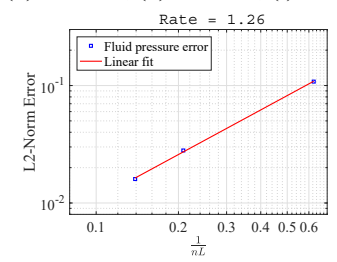


Figure 5: Convergence plot in $\|e\|_2$ for fluid pressure (n=4,12,18 and L=0.4 mm). The slope of the regression line is 1.26.

DISCUSSION

We established a 3-D multiscale homogenization scheme for fluid-saturated porous media. Our results demonstrate that size effects do influence results, e.g. distributions of stress and fluid pressure, within our multiscale solutions. However, the size effects are managable as we can make them arbitrarily small by increasing the difference in length scales between macro- and micro-scale models. As this difference increases, e.g. increasing n in 1/nL (n=4,12,18), the $\|e_p\|_2$ -norm error decreases with slope 1.26. Our FE2M framework (FE analyses augmented to derive the material behaviors from a distribution of finer scale FE analyses) facilitates studies of engineering materials for applications in biomedical engineering, material science, and environmental sciences. In particular, our FE2M framework is ideally suited to bridge the joint, tissue, and intratissue scales for problems in biomechanics, but has not yet been applied to multi-phase, fibrous soft tissues.

ACKNOWLEDGEMENTS

NSF CAREER 1653358; Gerard Ateshian and Steve Maas.

REFERENCES

- [1] Bowen RM. Int. J. Eng. Sci. 20.6 (1982).
- [2] Feyel F. Comput. Methods in Appl. Mech. Eng. 192.28-30 (2003).